

Contents lists available at ScienceDirect

# Bioresource Technology

journal homepage: www.elsevier.com/locate/biortech



# Effects of anodic oxidation of a substoichiometric titanium dioxide reactive electrochemical membrane on algal cell destabilization and lipid extraction



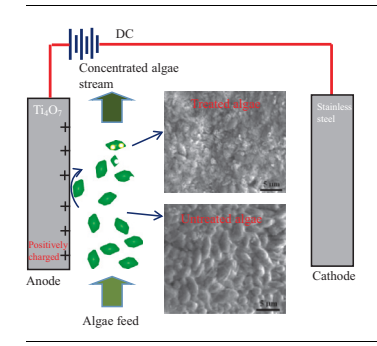
Likun Hua <sup>a</sup>, Lun Guo <sup>b</sup>, Megha Thakkar <sup>c</sup>, Dequan Wei <sup>d</sup>, Michael Agbakpe <sup>a</sup>, Liyuan Kuang <sup>a</sup>, Maraha Magpile <sup>a</sup>, Brian P. Chaplin <sup>b</sup>, Yi Tao <sup>d</sup>, Danmeng Shuai <sup>e</sup>, Xihui Zhang <sup>d</sup>, Somenath Mitra <sup>c</sup>, Wen Zhang a,\*

- <sup>a</sup> John A. Reif, Jr. Department of Civil & Environmental Engineering, New Jersey Institute of Technology, Newark, NJ 07102, United States
- <sup>b</sup>Department of Chemical Engineering, University of Illinois at Chicago, Chicago, IL 60607, United States
- <sup>c</sup> Department of Chemistry and Environmental Science, New Jersey Institute of Technology, Newark, NJ 07102, United States
- d Research Center of Environmental Engineering & Management, Graduate School at Shenzhen, Tsinghua University, Shenzhen 518055, PR China
- e Department of Civil and Environmental Engineering, The George Washington University, Washington, DC 20052, United States

#### HIGHLIGHTS

- Ti<sub>4</sub>O<sub>7</sub> REM could oxidize algal cells under anodic polarization.
- The anodic oxidation led to algal cell destabilization and damage.
- The lipid extraction efficiency was enhanced with the destabilized algal cells.
- REM filtration may potentially incorporate cell pretreatment for enhancing lipid extraction.

#### G R A P H I C A L A B S T R A C T



# ARTICLE INFO

Article history: Received 12 November 2015 Received in revised form 14 December 2015 Accepted 15 December 2015 Available online 18 December 2015

Keywords: Algal harvesting Algal pretreatment Membrane separation Lipid extraction

# ABSTRACT

Efficient algal harvesting, cell pretreatment and lipid extraction are the major steps challenging the algal biofuel industrialization. To develop sustainable solutions for economically viable algal biofuels, our research aims at devising innovative reactive electrochemical membrane (REM) filtration systems for simultaneous algal harvesting and pretreatment for lipid extraction. The results in this work particularly demonstrated the use of the Ti<sub>4</sub>O<sub>7</sub>-based REM in algal pretreatment and the positive impacts on lipid extraction. After REM treatment, algal cells exhibited significant disruption in morphology and photosynthetic activity due to the anodic oxidation. Cell lysis was evidenced by the changes of fluorescent patterns of dissolved organic matter (DOM) in the treated algal suspension. The lipid extraction efficiency increased from  $15.2 \pm 0.6$  g-lipid g-algae<sup>-1</sup> for untreated algae to  $23.4 \pm 0.7$  g-lipid g-algae<sup>-1</sup> for treated algae (p < 0.05), which highlights the potential to couple algal harvesting with cell pretreatment in an integrated REM filtration process.

© 2015 Elsevier Ltd. All rights reserved.

### 1. Introduction

Algal biomass is the third generation feedstock for biodiesel or biofuel production. However, expensive algal harvesting, biomass

<sup>\*</sup> Corresponding author. Tel.: +1 973 596 5520; fax: +1 973 596 5790. E-mail address: wzhang81@njit.edu (W. Zhang).

pretreatment, and lipid extraction represent the major hurdles for producing cheap biofuels at industrial scales. Typical structures of algal cell walls contain uronic acids, glucosamine, and polysaccharides that provide cells with formidable defense against environmental conditions (Scholz et al., 2014). Extraction of biolipid that is usually located in globules or bound to cell membranes often involves the use of organic solvents such as n-hexane, chloroform and methanol because of their high selectivity and solubility towards lipids (Cheng et al., 2011; Lee et al., 2010). An efficient extraction requires that the solvent penetrates completely into the biomass and physically contacts the lipid (e.g., triglyceridesesters) located in the photosynthetically active membranes. Therefore, cell disruption is a necessary pretreatment step prior to lipid extraction.

Cell disruption and lipid extraction processes can be energyintensive, time-consuming and costly. Current cell disruption methods include mechanical and non-mechanical techniques. Mechanical techniques destroy the cell wall using non-specific solid and liquid shear forces or energy transfer through heating and waves (Günerken et al., 2015), which include compression, high-pressure homogenization (HPH) (Park et al., 2015), ultrasonic bath (Greenly and Tester, 2015), autoclave (Lee et al., 2010), bead mill, microwave and magnetic stirring (Cravotto et al., 2008; Virot et al., 2008); while non-mechanical techniques include chemical lysing using enzymes or chemical agents and osmotic shock (Demuez et al., 2015; Harun et al., 2011). Selective interactions between chemical agents (enzymes, antibiotics, chelating agents, chaotropes, detergents, hypochlorite, acids and alkali) and the cell wall or membrane are designed to facilitate biolipid leaching (Günerken et al., 2015). Life-cycle assessment (LCA) of biofuel production from microalgae feedstock determined that cultivation, harvesting and lipid extraction accounted for up to 90% of the total process energy (Brentner et al., 2011). Further decreasing solvent consumption, preventing pollution, and enhancing lipid production (efficiency) are the major challenges in this field.

Reactive electrochemical membranes (REMs) based on electrochemical advanced oxidation processes (EAOPs) are a cuttingedge class of membranes that hold great promise in revolutionizing water/wastewater treatment and bioseparation processes (Zaky and Chaplin, 2013). REMs are porous three-dimensional electrodes that can provide anodic oxidation in addition to physical separation (Liu and Vecitis, 2011; Zaky and Chaplin, 2013). Hydroxyl radicals (OH') form via water oxidation when the REM is anodically polarized (Zaky and Chaplin, 2013). Recent work has shown that porous substoichiometric TiO<sub>2</sub> (e.g., Ti<sub>4</sub>O<sub>7</sub>) anodes were operated in a cross-flow filtration mode, leading to a combination of microfiltration and electrochemical oxidation (Zaky and Chaplin, 2014, 2013). By converting TiO<sub>2</sub> to Ti<sub>4</sub>O<sub>7</sub> (usually at temperatures above 900 °C under a H<sub>2</sub> atmosphere) (Chen et al., 2002), electrical conductivity can be increased from  $10^{-9} \Omega^{-1} \text{ cm}^{-1}$  (TiO<sub>2</sub>) as high as  $166 \Omega^{-1} \text{ cm}^{-1}$  (Ti<sub>4</sub>O<sub>7</sub>). Thus, the REM has shown promising antifouling properties, as adsorbed organic foulants were shown to be removed via the anodic oxidation process (Zaky and Chaplin, 2014). The micrometer-sized pores of the REM produced a high electroactive surface area and advection-enhanced mass transfer rates approximately 10-fold higher than those obtained in traditional flow-by mode. Past research with REMs has focused largely on dissolved compound oxidation, but their ability to separate or pretreat microbial cells such as algae is unexplored. Meanwhile, it is also important to compare the cost effectiveness with traditional membranes or other separation techniques.

Our overall research aim is to explore substoichiometric  ${\rm TiO_2}$  REMs for efficient algal harvesting and pretreatment while maintaining high flux during filtration and excellent stability under anodic and cathodic polarization. In this work we specifically explored the effect of REM anodic potential on algal cell integrity and the

effect of algal disruption on lipid extraction efficiency. Our hypothesis is that algal cells, upon exposure to polarized REM surfaces, could be oxidized and destabilized, which may positively increase the downstream lipid extraction efficiency if properly controlled in terms of exposure time and REM polarization. The produced OH and other oxidative species will likely contribute to the algal cell oxidation. The oxidative disruption of cell integrity was evaluated using various characterization techniques (e.g., optical and electron microscopes, atomic force microscope, measurements of photosynthetic activity and oxygen production), and the influence of cell disruption on the biolipid extraction efficiency is assessed in order to shed new insights into the potential synergistic benefits of the REM in algal harvesting and pretreatment.

#### 2. Methods

#### 2.1. Substoichiometric TiO<sub>2</sub> REM

The REM used in this study is a 10-cm long Ebonex® one-channel tubular electrode with the outer and inner diameters of 10 mm and 6 mm, respectively (Vector Corrosion Technologies, Inc.). Ebonex is a Magneli phase suboxide of TiO2, which consists primarily of Ti5O9 and Ti4O7. Synthesis and characterization of the REM was reported previously (Zaky and Chaplin, 2013), which showed an average pore diameter of 1.70  $\pm$  0.02  $\mu m$ , a porosity of 30.7  $\pm$  2.8% and a specific surface area of 2.8  $\pm$  0.7 m² g $^{-1}$ . As received Ebonex electrodes were subjected to a high temperature reduction treatment (1 atm H2, 1050 °C, 4 h) to produce high purity Ti4O7. The X-ray Diffraction pattern and scanning electron microscope (SEM) data were acquired to analyze crystallinity and morphology of the prepared REM.

#### 2.2. Algal cultivation and preparation

Oleaginous algae (*Scenedesmus dimorphus* or *S. dimorphus*) were cultivated in the modified Bold's Basal Medium (MBBM) with details reported in our previous works (Agbakpe et al., 2014; Ge et al., 2014, 2015). Briefly, *S. dimorphus* was cultivated in 2-L Erlenmeyer flasks and at the room temperature ( $25 \pm 1$  °C), with CO<sub>2</sub> fed at a rate of  $8.5 \times 10^{-4}$  L-CO<sub>2</sub> min<sup>-1</sup>.(L-medium)<sup>-1</sup>. The light–dark cycle (12 h/12 h) was maintained at a photon flux of approximately 4200 mW m<sup>-2</sup> as measured by a spectroradiometer (Spectral Evolution, SR-1100). The algal concentration (g L<sup>-1</sup>) was characterized by the dry cell weight (DCW). The steady-state algal concentration after 14-day incubation was around 1.4 g L<sup>-1</sup>, which was then used for algal harvesting experiments and other tests.

## 2.3. REM exposure experiments

To study the cell damage as a function of the charge passed through the REM, a batch electrochemical reaction cell was used to simulate the algal cell exposure with REM during the crossflow filtration process. The reaction cell was filled with the algal suspension, and the REM was positioned in the middle of the reactor (anode) and was surrounded by a stainless steel circular mesh (cathode) with a spacing of 2.5 cm. The REM was operated at a constant current (100-500 mA) using a DC power supply (Proteck P6035, Tempe, AZ) corresponding to cell voltages between 10 and 20 V and for different times (30-120 min) to achieve different algal disruption. The effective exposure surface area of the REM was 25.4 cm<sup>2</sup>. The conductivity of the pure algal medium was  $1040 \pm 5 \,\mu\text{S cm}^{-1}$ , whereas the conductivity of the algal medium with growing algal cells ranged from  $1580 \pm 20$  to  $2520 \pm 10$ μS cm<sup>-1</sup> for newly inoculated algal cultures and cultures after 14 days of incubation, respectively.

#### 2.4. Cell disruption characterization

### 2.4.1. Morphology and surface composition

Cell morphology was examined by a fluorescent microscope (3012 Series, Miller Microscopes, Feasterville, PA), a Keysight 8500B scanning electron microscope (SEM), and an atomic force microscope (AFM) on a NTEGRA Prima AFM (NT-MDT Inc., Tempe, AZ). Briefly, The algal cells were inoculated with 2.5% (v/v) glutaraldehyde for 30 min and washed with phosphate buffer solution (PBS, 10 mM, pH 7.4) for 3 times. 100  $\mu L$  of the algal suspension was dropped onto the clean silicon wafer and air dried for 10 min, followed by the SEM or AFM observation. The surface compositions of untreated and treated algal cells, after air drying, were assessed by a Fourier Transform Infrared (FTIR) Spectrometer on a Nicolet ThermoElectron FTIR spectrometer.

#### 2.4.2. Algal photosynthetic activity

Algal growth activity or photochemical function was evaluated with photochemical parameters of phohtosystem II (PSII). PSII photochemical parameters were recorded by subjecting aliquots of the cultures to dark-adaption (10-min) followed by fluorescence induction and relaxation characterization using Satlantic FIRe System (Satlantic, Inc) under single turnover flash protocol. The protocol generates PSII maximum quantum yield (Fv/Fm) that could serve as an indicator of algal growth activity. Briefly, 25  $\mu L$  of algal suspension was taken and stabilized in the dark for 10 min. Then, 2 mL of media was added to the algal suspension, which was then subjected to the fluorescence measurement immediately. Moreover, the specific oxygen production rate (SOPR) was monitored to determine phototrophic activity of algae.

## 2.4.3. Changes of dissolved organic matter (DOM) in algal medium

DOM in algal suspension could originate from the released extracellular polymeric substances (EPS) from algae. Particularly for the damaged or lysed algae, cytoplasm could be released, leading to changes of the DOM types and concentrations. DOM was characterized by a Thermo scientific Evolution 201PC UV-vis spectrophotometer and a Hitachi FL4500 fluorescent spectrophotometer. The algal suspension was first centrifuged at 10,000g for 15 min to remove suspended algae or other large debris. The supernatant was then tested in a quartz cuvette by the UV-vis and florescence spectrophotometer. The UV-vis and fluorescent spectra as well as the 3D excitation/emission matrix (EEM) spectra were all obtained. Deionized (DI) water blanks were run to monitor the instrument stability.

### 2.4.4. Molecular weight (MW) distribution of DOM

The MW distribution of DOM was analyzed by high performance liquid chromatography (HPLC). HPLC used an HPSEC (LC-20AT, Shimadzu, Japan) system with the combination of a TSK gel G3000PWXL column (0.78 cm  $\times$  30 cm) and a TSK gel G2500PWXL column (0.78 cm  $\times$  30 cm) in series. The HPSEC was coupled to a photodiode array detector (SPD-M20A, Shimadzu, Japan) and an on-line TOC detector (TOC, Sievers 900 Turbo TOC, GE, USA). The mobile phase was a phosphate buffer (2.4 mmol L $^{-1}$  NaH<sub>2</sub>PO<sub>4</sub> and 1.6 mmol L $^{-1}$  Na<sub>2</sub>HPO<sub>4</sub>) and 25 mmol L $^{-1}$  Na<sub>2</sub>SO<sub>4</sub>. The flow rate was 0.5 mL min $^{-1}$ . Sodium polystyrene sulfonate standards (34,700, 10,600, 6800, 4300 and 1670 Da, PSS Polymer Standards Service GmbH, Germany) were used to calibrate the MW distribution. The supernatant of the algal suspension was filtered through 0.45- $\mu$ m polyethersulfone membranes prior to injection into the HPLC.

#### 2.5. Lipid extraction

The untreated and treated algal biomass was vacuum dried at room temperature prior to the solvent extraction (Pragya et al.,

2013). To extract lipid, aliquots (*ca.* 0.5 g) of dried algal biomass were extracted with 40 mL of 2:1 dichloromethane:methanol with 400-W microwave irradiation for 45 min, and then centrifuged at 1000g for 15 min. The supernatant was transferred into a preweighed test tube while the pellet was successively reextracted with a 1:1 and then a 1:2 dichloromethane: methanol solution. The supernatant from each step was transferred to the same test tube. DI water (50 mL) was added to the test tube and incubated at 4 °C overnight. The lower organic layer was collected and evaporated using a Thermo Savant AES1010 Automatic Environmental Speedvac system (Thermo Fisher Scientific, Waltham, MA). Dry weights of the samples were determined. Lipid content was calculated by dividing the dry weight of the extracted lipid by the dry weight of the samples used for lipid extraction (g-lipid g-algae<sup>-1</sup>).

## 2.6. Statistical analysis

Algal treatment experiments were carried out in duplicate for each condition. Filtration and lipid extraction were performed in duplicate or higher. The presented results are mean values  $\pm$  standard deviation from three independent experiments. The differences between experimental groups and control groups were tested for significance using one-way analysis of variance (ANOVA) at a 5% significance level (p = 0.05).

#### 3. Results and discussion

# 3.1. Algal morphological changes and possible algal disruption mechanisms

Cell disruption was revealed by both SEM and AFM images. Untreated algae remained intact and in normal shapes, whereas treated algae cells deformed and had rough surfaces. Some cell debris or intracellular substances were released, which was previously observed during algal lysis after ozonation treatment (Hung and Liu, 2006). Algal suspension shifted from dark green to lighter green over the time of REM treatment. The color of the dried algal biomass also shifted from dark black to light black. Optical microscope images did not indicate any major changes to the morphology of algal cells. However, white-colored dots were found on the treated algae, which could be the pits (cavitation) on the damaged algal cell wall (Günerken et al., 2015).

The observed cell damage, disruption, and decolorization of algal suspensions were likely due to the anodic oxidation of algae and algogenic organic matters (AOM) either by reactive oxygen species (e.g., 'OH) or direct oxidation at the REM. However, other potential oxidant sources in our batch reactor include the formation of  $\rm H_2O_2$  on the stainless steel cathode and  $\rm Cl_2$  at the REM anode. The  $\rm H_2O_2$  concentration at an applied current of 500 mA for 2 h (1 A h) was determined to be 8 ± 2  $\mu$ M, which should have negligible effects on algal cell oxidation in our case. A recent study showed only small increases in lipid extraction due to *Chlorella vulgaris* cell oxidation with  $\rm H_2O_2$  concentrations of 0.2–1.5 M. The total chloride concentration in algal medium was 0.8 mM so that a maximum level of 0.4 mM Cl<sub>2</sub> could be produced at the anode surface, and therefore may contribute to algal cell oxidation (Steriti et al., 2014).

#### 3.2. Algal surface functional groups

Surface disruption may also lead to the disintegration of extracellular organic matter (EOM) from the algal surface. FTIR was utilized to examine the effect of REM treatment on algal surface functional groups. Typical components on algal surfaces are polysaccharides, proteins, lipids, and phosphate groups. The char-

acteristic peaks at 3550-3200, 2925, 1260-1000 cm<sup>-1</sup> are associated with polysaccharide or polysaccharide-like substances, such as N-H stretching occurred at 3300 cm<sup>-1</sup>, aliphatic (-CH<sub>2</sub>) peak at 2930 cm<sup>-1</sup>, carboxylic (C-O) at 1250 cm<sup>-1</sup> and 1000 cm<sup>-1</sup> (Hung and Liu, 2006). The absorption peaks at 1650 cm<sup>-1</sup> and 1550 cm<sup>-1</sup> are related to the peptide carbonyls (C=O, amide I band) and the N-H (amide II) bonding, respectively (Qu et al., 2012). FTIR spectra indicated that protein and polysaccharidelike substances were major constituents on the surface of S. dimorphus. All major functional groups remained with their intensities slightly decreasing as a result of REM treatment, implying EOM (e.g., polysaccharides) were likely released from the algal surface due to the oxidant attack on the cell wall of algae and subsequently algal lysis. Furthermore, similar changes in cell surface characteristics and in cell viability upon addition of oxidants was observed in previous works (Hung and Liu, 2006).

#### 3.3. Algal photosynthetic activity changes

Fig. 1 compares four photosynthetic efficiency curves for untreated and treated algae under three different electrochemical treatment times (500 mA and 20 V) in 500 mL. The photosynthetic efficiency declined from 0.5 to 0.2 fv fm<sup>-1</sup> with the increase of the treatment time from 0 to 120 min (2.0 A h  $L^{-1}$ ). The experimental determination of dissolved oxygen (DO) regeneration curves were generated for untreated and treated algae under two different conditions, as an indicator of algal photosynthetic activity. Clearly, the DO curve for the untreated algae was highly linear ( $R^2 = 0.98$ ) at a rate of c.a.  $2.7 \text{ mg L}^{-1} \text{ h}^{-1}$ , which is the greatest among the three samples. By applying 100 mA and 10 V to the REM to treat algae suspension of 500 mL for 60 min (0.2 A h L<sup>-1</sup>), the treated algae maintained the similar photosynthetic activity with the untreated algae. However, further increasing the DC level to 500 mA and 20 V  $(2.0 \text{ A h L}^{-1} \text{ or } 20 \text{ W L}^{-1})$ , the REM exposure significantly inhibited DO regeneration due to the cell damage or lysis.

#### 3.4. Characterization of DOM in algal suspension

Polysaccharide-like and protein-like substances found on the algal surfaces were likely the major components of AOM released from algae due to surface oxidation. In addition, cell lysis by oxidation may also cause a release of intracellular organic matter (IOM) that is considered as hydrophilic substances with high SUVA<sub>254</sub>, the ratio of UV<sub>254</sub> to dissolved organic carbon (DOC). To evaluate the possible algal surface oxidation by the REM treatment, the UV-vis spectra for the supernatant collected from untreated and

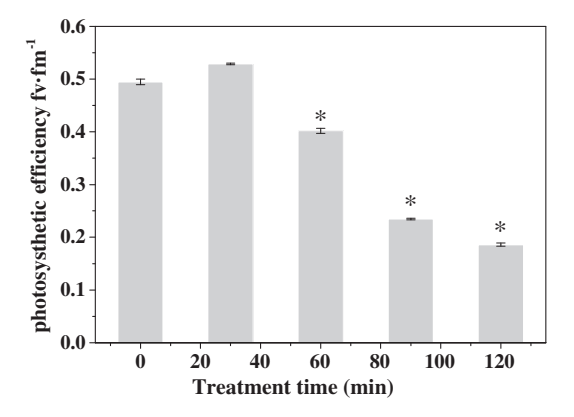


**Fig. 1.** Photosynthetic activity for the untreated and treated algal cells under the condition: 500 mA (current density  $\approx$  20 mA cm<sup>-2</sup>) and 20 V for 500 ml of algal suspension at the initial concentration of 1.4 g L<sup>-1</sup>. \*denotes significant differences (p < 0.05) between the values of treatment groups and the initial value.

treated algal suspensions were obtained. The data shows little difference between the samples, which is likely due to the low concentrations of AOM in the algal suspensions.

However, the EEM spectra obtained by the fluorescent spectrophotometer shown in Fig. 2 were able to resolve the changes in protein and humic- or fulvic-like substances in algal suspensions. There were two major peaks at Ex/Em of 245/400 nm and 340/400 nm. After the treatment, a peak at (Ex/Em of 350 nm/400 nm) emerged, which is likely ascribed to humic substances. This may indicate that the production or release of AOM from algae was due to anodic oxidation. It was previously reported that DOC in the algal suspension increased as contact time of ozonation increased (Hung and Liu, 2006). Ozone exposure further reduced the algal mass and the size of algal cells due to the release of AOM from algal surfaces. Consequently, the fluorescent intensity of the observed peaks in EEM also decreased, which agreed with the FTIR results.

The MW distribution of DOM usually exhibits a significant heterogeneity (high polydispersity) due to an array of different components such as carbohydrates, polysaccharides, amino acids, peptides, and enzymes (Her et al., 2004). Carbohydrates or proteins have high MW (>20 kDa), while humic like substances have medium MW of a few kDa with some building blocks of 350-500 Da or less. The MW distribution ranged from 1.8 kDa to 2.6 kDa and did not reveal any high MW biopolymers probably due to the limited resolving power of HPLC detectors for DOM. There were two peaks at 2.6 kDa and 1.8 kDa for the untreated algal medium, which both decreased likely due to the decomposition of typical AOM. The smaller peak at 2.1 kDa increased for the treated algal medium implying a possible conversion of larger organic compounds to smaller ones as a result of oxidation. This shift can be verified by the UV absorbance ratio index (URI) and  $S_{250-365}$ . URI is the ratio of UV absorbance at 210 nm to that at 254 nm (UVA<sub>210</sub>/UVA<sub>254</sub>), which indicates the relative proportions between UV-absorbing functional groups and unsaturated compounds in DOM (a higher URI means a smaller MW of DOM) (Uyguner and Bekbolet, 2005). The  $S_{250-365}$  is a spectral absorption index equal to the spectral slope coefficient in the spectral range of 250-365 nm as shown in Eq. (S1), which indicates the MW range of DOM (a higher S<sub>250-365</sub> indicates a lower MW) (Helms et al., 2008). Based on the UV-vis spectral data, URI and S<sub>250-365</sub> were calculated and found to increase after the REM treatment, indicating that new DOM of low-range MW emerged in treated algal suspensions due to the cell lysis and the release of AOM.

#### 3.5. Lipid extraction efficiency

The specific extracted lipid increased from  $15.2 \pm 0.6$  to  $23.4 \pm 0.7$  g-lipid g-cells<sup>-1</sup> (p < 0.05) as the REM treatment intensity increased from 0 to 0.75 A h by increasing the exposure time at 500 mA. Clearly, the REM treated cells allowed greater lipid extraction efficiencies presumably due to the oxidative cell damage. Similar improvement in lipid extraction was previously reported when other algal pretreatment such as pressure-assisted ozonation (PAO), Fenton oxidation, and peroxone treatment were applied (Huang et al., 2014; Nguyen et al., 2013).

# 3.6. Comparison of energy consumption with other algal pretreatment techniques

Algal pretreatment by anodic oxidation of REM is comparable to the above-mentioned techniques such as ultrasonication, microwave, or pulsed electric field (PEF) charging, which employ oxidative stress or an electrical field to induce membrane compression or cavity formation to facilitate lipid extraction. Mechanical techniques, such as bead mill, high-pressure homogenization (HPH)

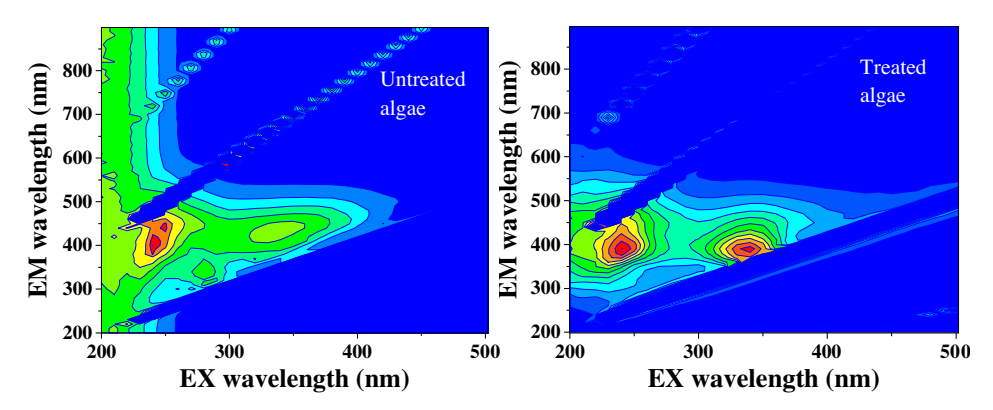


Fig. 2. EEM spectra for the supernatant from untreated and treated algal suspension under the condition: 500 mA (current density  $\approx$  20 mA cm<sup>-2</sup>), 20 V and 60 min for 500 mL of algal suspension at the initial concentration of 1.4 g L<sup>-1</sup>. The intensity of EEM is represented by contour lines.

and high speed homogenizer (HSH), consume nearly the same amount of energy to process a unit of volume, independent on whether the feed is diluted or concentrated (Zbinden et al., 2013). Thus, for these methods, processing higher DCW concentrations per unit of time is more cost effective. Energy consumption not only varies with processes but also design parameters. For example. Doucha and Lívanský reported that the specific energy consumption (kW h/kg-disrupted cells) of bead milling can be reduced from 10.3 to 0.86 kW h kg<sup>-1</sup> by changing the process parameters (Doucha and Lívanský, 2008). Energy consumption also does not scale with algal cell numbers, as a recent study on the disruption of Tetraselmis suecica through AFM measured an energy consumption of 0.000187 kW h kg<sup>-1</sup> to break up a single cell on the analytical scale. Several authors compared different methods at low DCW concentrations, i.e., ultrasonication, HPH, bead milling and microwave treatment (Halim et al., 2012; Lee et al., 2012, 2010). Generally, HPH has the highest specific energy consumption, followed by microwave treatment and ultrasonication. Ultrasonication has a specific energy consumption ranging from  $36.67 \text{ kW h kg}^{-1}$  (inefficient disruption) to  $100 \text{ kW h kg}^{-1}$  (efficient disruption) (Halim et al., 2012; Lee et al., 2010). For continuous PEF treatment processes, the specific energy consumption almost linearly decreases with the biomass treatment rate (kg  $h^{-1}$ ), i.e., biomass disrupted per unit of time (Coustets et al., 2013). In other words, specific energy demand strongly depends on the concentration of the suspension and ranges from 0.42 kW h kg<sup>-1</sup> for 10% DCW to 239 kW h  $kg^{-1}$  for 0.03% DCW (Sheng et al., 2012, 2011). A recent literature review suggested that algal biomass preprocessing should not exceed a threshold level of energy consumption (5.8 kW h kg<sup>-1</sup>) in order to be cost effective (Günerken et al., 2015). Our current bench scale algal treatment by REM had a relatively high-energy consumption of approximately 28.6 kW h kg<sup>-1</sup> to achieve improved lipid extraction from approximately 15-23%. However, it is worth mentioning that the REM treatment can further be optimized (e.g., reducing the electrode spacing from 2.5 cm to 0.5 cm), which may reduce the needed cell voltages from 20 V to 4 V while maintaining the same current density. Moreover, one should keep in mind that the use of REM filtration is primarily for efficient algal harvesting with potential to reduce membrane fouling under anodic polarization and to enable the reuse of permeate water and nutrients. Thus, it may not be necessary to directly compare energy consumption or cost between REM and other algal cell pretreatment techniques.

#### 4. Conclusion

Algal cells underwent significant disruption in morphology under anodic oxidation by a  ${\rm Ti_4O_7}$  REM. The REM-treated algae

had reduced photosynthetic activity and oxygen production rates compared to untreated algal cells. Algal lysis was evidenced by the release of AOM that was characterized by EEM, HPLC, and UV-vis spectrometry. This work demonstrated for the first time the use of a novel REM to oxidize algal cells, which resulted in an increase in the lipid extraction efficiency. Overall, the results offered new insights into the design of innovative REM systems for integrated algal biomass separation and cell treatment for biofuel production.

# Acknowledgements

This study was supported by the Research Startup Fund at NJIT and National Science Foundation Grant CBET-1235166. Authors are thankful to the support of XRD analysis by the Faculty Instrument Usage Seed Grant (FIUSG) from the Otto York Center and the Materials Characterization Lab at NJIT, Mr. Maocong Hu and Prof. Xianqin Wang's support in FTIR analysis, Penghui Li from Tongji University for the discussion on EEM data interpretation, and NT-MDT America Inc. for the AFM characterization. Prof. Brian P. Chaplin and Mr. Lun Guo were partially supported by National Science Foundation grants CBET-1159764 and CBET-1453081 (CAREER).

#### Appendix A. Supplementary data

Supplementary data associated with this article can be found, in the online version, at http://dx.doi.org/10.1016/j.biortech.2015.12.041.

#### References

Agbakpe, M., Ge, S., Zhang, W., Zhang, X., Kobylarz, P., 2014. Algae harvesting for biofuel production: influences of uv irradiation and polyethylenimine (PEI) coating on bacterial biocoagulation. Bioresour. Technol. 166, 266–272.

Brentner, L.B., Eckelman, M.J., Zimmerman, J.B., 2011. Combinatorial life cycle assessment to inform process design of industrial production of algal biodiesel. Environ. Sci. Technol. 45, 7060–7067.

Chen, G., Bare, S.R., Mallouk, T.E., 2002. Development of supported bifunctional electrocatalysts for unitized regenerative fuel cells. J. Electrochem. Soc. 149, A1092–A1099.

Cheng, C.H., Du, T.B., Pi, H.C., Jang, S.M., Lin, Y.H., Lee, H.T., 2011. Comparative study of lipid extraction from microalgae by organic solvent and supercritical CO<sub>2</sub>. Bioresour. Technol. 102, 10151–10153.

Coustets, M., Al-Karablieh, N., Thomsen, C., Teissié, J., 2013. Flow process for electroextraction of total proteins from microalgae. J. Membr. Biol. 246, 751–760

Cravotto, G., Boffa, L., Mantegna, S., Perego, P., Avogadro, M., Cintas, P., 2008. Improved extraction of vegetable oils under high-intensity ultrasound and/or microwaves. Ultrason. Sonochem. 15, 898–902.

Demuez, M., Mahdy, A., Tomás-Pejó, E., González-Fernández, C., Ballesteros, M., 2015. Enzymatic cell disruption of microalgae biomass in biorefinery processes. Biotechnol. Bioeng.

- Doucha, J., Lívanský, K., 2008. Influence of processing parameters on disintegration of chlorella cells in various types of homogenizers. Appl. Microbiol. Biotechnol. 81, 431–440.
- Ge, S., Agbakpe, M., Wu, Z., Kuang, L., Zhang, W., Wang, X., 2014. Influences of surface coating, UV irradiation and magnetic field on the algae removal using magnetite nanoparticles. Environ. Sci. Technol. 49, 1190–1196.
- Ge, S., Agbakpe, M., Zhang, W., Kuang, L., 2015. Heteroaggregation between PEI-coated magnetic nanoparticles and algae: effect of particle size on algal harvesting efficiency. ACS Appl. Mater. Inter. 7, 6102–6108.
- Greenly, J.M., Tester, J.W., 2015. Ultrasonic cavitation for disruption of microalgae. Bioresour. Technol. 184, 276–279.
- Günerken, E., D'Hondt, E., Eppink, M.H.M., Garcia-Gonzalez, L., Elst, K., Wijffels, R.H., 2015. Cell disruption for microalgae biorefineries. Biotechnol. Adv. 33, 243–260.
- Halim, R., Harun, R., Danquah, M.K., Webley, P.A., 2012. Microalgal cell disruption for biofuel development. Appl. Energy 91, 116–121.
- Harun, R., Jason, W., Cherrington, T., Danquah, M.K., 2011. Exploring alkaline pretreatment of microalgal biomass for bioethanol production. Appl. Energy 88, 3464–3467.
- Helms, J.R., Stubbins, A., Ritchie, J.D., Minor, E.C., Kieber, D.J., Mopper, K., 2008. Absorption spectral slopes and slope ratios as indicators of molecular weight, source, and photobleaching of chromophoric dissolved organic matter. Limnol. Oceanogr. 53, 955–969.
- Her, N., Amy, G., Park, H.-R., Song, M., 2004. Characterizing algogenic organic matter (AOM) and evaluating associated NF membrane fouling. Water Res. 38, 1427–1438
- Huang, Y., Hong, A., Zhang, D., Li, L., 2014. Comparison of cell rupturing by ozonation and ultrasonication for algal lipid extraction from *Chlorella vulgaris*. Environ. Technol. 35, 931–937.
- Hung, M., Liu, J., 2006. Microfiltration for separation of green algae from water. Colloids Surf. B 51, 157–164.
- Lee, J.Y., Yoo, C., Jun, S.Y., Ahn, C.Y., Oh, H.M., 2010. Comparison of several methods for effective lipid extraction from microalgae. Bioresour. Technol. 101, S75–S77.
- Lee, A.K., Lewis, D.M., Ashman, P.J., 2012. Disruption of microalgal cells for the extraction of lipids for biofuels: processes and specific energy requirements. Biomass Bioenergy 46, 89–101.
- Liu, H., Vecitis, C.D., 2011. Reactive transport mechanism for organic oxidation during electrochemical filtration: mass-transfer, physical adsorption, and electron-transfer. J. Phys. Chem. C 116, 374–383.

- Nguyen, T.L., Lee, D., Chang, J., Liu, J., 2013. Effects of ozone and peroxone on algal separation via dispersed air flotation. Colloids Surf. B 105, 246–250.
- Park, J.-Y., Park, M.S., Lee, Y.-C., Yang, J.-W., 2015. Advances in direct transesterification of algal oils from wet biomass. Bioresour. Technol. 184, 267–275.
- Pragya, N., Pandey, K.K., Sahoo, P., 2013. A review on harvesting, oil extraction and biofuels production technologies from microalgae. Renew. Sustain. Energy Rev. 24, 159–171.
- Qu, F., Liang, H., Tian, J., Yu, H., Chen, Z., Li, G., 2012. Ultrafiltration (UF) membrane fouling caused by cyanobateria: fouling effects of cells and extracellular organics matter (EOM). Desalination 293, 30–37.
- Scholz, M.J., Weiss, T.L., Jinkerson, R.E., Jing, J., Roth, R., Goodenough, U., Posewitz, M. C., Gerken, H.G., 2014. Ultrastructure and composition of the *Nannochloropsis gaditana* cell wall. Eukaryot. Cell 13, 1450–1464.
- Sheng, J., Vannela, R., Rittmann, B.E., 2011. Evaluation of cell-disruption effects of pulsed-electric-field treatment of synechocystis PCC 6803. Environ. Sci. Technol. 45, 3795–3802.
- Sheng, J., Vannela, R., Rittmann, B., 2012. Disruption of synechocystis PCC 6803 for lipid extraction. Water Sci. Technol. 65, 567–573.
- Steriti, A., Rossi, R., Concas, A., Cao, G., 2014. A novel cell disruption technique to enhance lipid extraction from microalgae. Bioresour. Technol. 164, 70–77.
- Uyguner, C.S., Bekbolet, M., 2005. Evaluation of humic acid photocatalytic degradation by UV-vis and fluorescence spectroscopy. Catal. Today 101, 267– 274.
- Virot, M., Tomao, V., Ginies, C., Visinoni, F., Chemat, F., 2008. Microwave-integrated extraction of total fats and oils. J. Chromatogr. A 1196, 57–64.
- Zaky, A.M., Chaplin, B.P., 2013. Porous substoichiometric TiO<sub>2</sub> anodes as reactive electrochemical membranes for water treatment. Environ. Sci. Technol. 47, 6554–6563.
- Zaky, A.M., Chaplin, B.P., 2014. Mechanism of p-substituted phenol oxidation at a  $Ti_4O_7$  reactive electrochemical membrane. Environ. Sci. Technol. 48, 5857–5867.
- Zbinden, M.D.A., Sturm, B.S., Nord, R.D., Carey, W.J., Moore, D., Shinogle, H., Stagg-Williams, S.M., 2013. Pulsed electric field (PEF) as an intensification pretreatment for greener solvent lipid extraction from microalgae. Biotechnol. Bioeng. 110, 1605–1615.